Supporting Information

A Cucurbit[8]uril-mediated Host-guest Complex for Red Light Photocatalysis.

Weiquan Xu*, Yinghao Du, He Ma, Xingchen Tang, Jiang-Fei Xu, Xi Zhang*.

Email: xwq19@mails.tsinghua.edu.cn;xi@mail.tsinghua.edu.cn

Content:

1. Material and methods.

All chemicals used in this research were purchased from commercial suppliers without further purification.

The ^{1}H NMR spectra were obtained using a JOEL JNM-ECA400 or Bruker 500 MHz AVANCEIIIHD with a cryoprobe. The UV-Vis spectra were collected using a HITACHIU-3010 spectrophotometer. The fluorescence spectra were collected using Edinburgh FLS1000 Photoluminescence Spectrometer. The fluorescence lifetime was measured using an Edinburgh LifeSpec II with Taiko laser. The nanosecond transient absorption spectra were measured by Edinburgh LP-980-KS spectrophotometer with a Continuum laser at 520 nm for excitation. Electrospray ionization mass spectrometry (ESI-MS) was carried out on a LCMS-IT/TOF (Shimadzu, Japan) system. Isothermal titration calorimetry (ITC) experiments were carried out with the Microcal VP-ITC apparatus at 298.15 K.

2. Synthesis and Characterization.

Synthesis of TPP: MPT was synthesized according to the literature[1]. 2.0 mmol MPT and 10 equivalents of 1-Chloro-2,4-dinitrobenzene were added in 100 mL ethyl alcohol. MPT-NO_2 was obtained by filtration after reacting for half a month at 90 ^{o}C. 0.5 mmol MPT-NO_2 was dissolved in 20 mL ethyl alcohol, and 2.2 equivalents of 6-pyrrolidin-1-ylpyridin-3-amine in 10 mL ethyl alcohol was added by using dropping funnel. After reacting for about 12 h, the solution was added into the mixing solution containing 60 mL ethyl ether and 30 mL acetone. The target product was obtained by filtration and washed with distilled water very carefully.

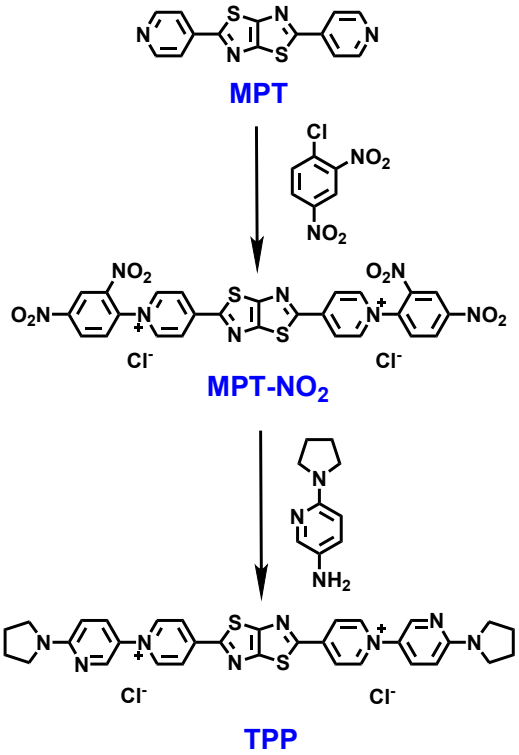

Figure S1. The synthesis of TPP.

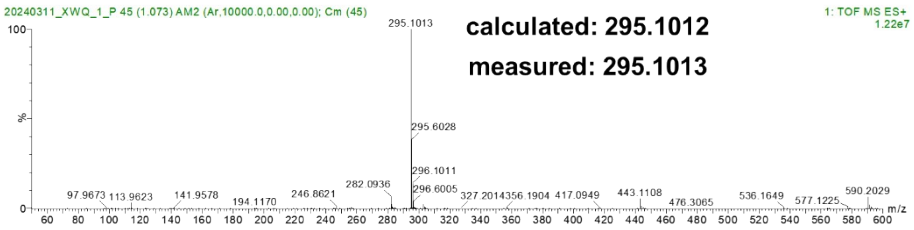

Figure S2. ESI-IT/TOF mass spectrum of TPP.

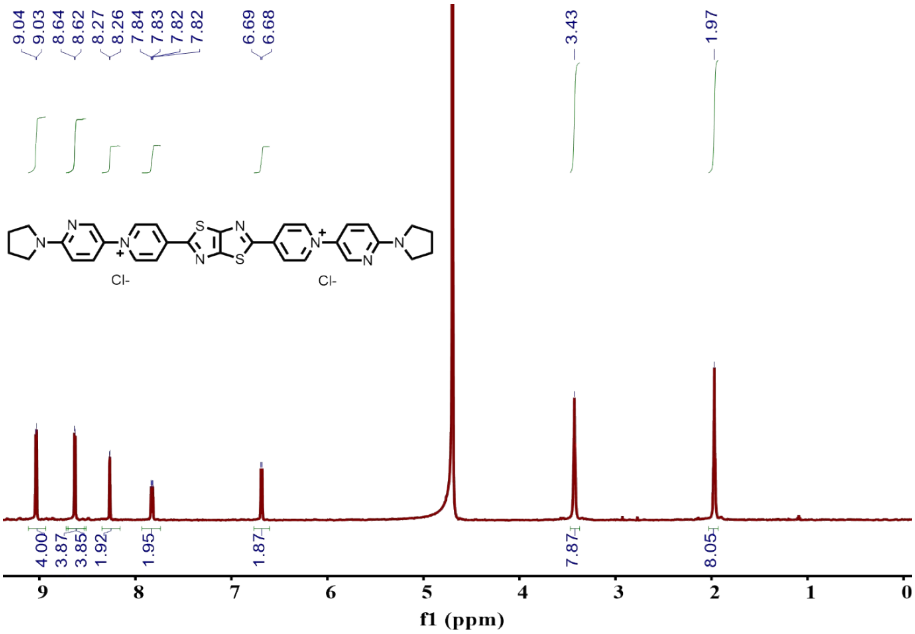

Figure S3. ^{1}H NMR spectrum of TPP.

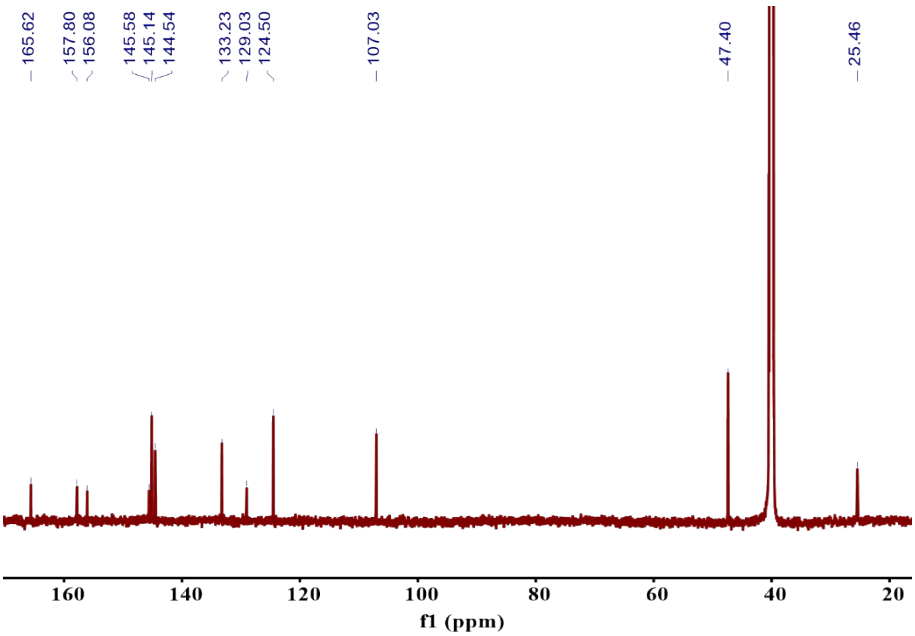

Figure S4. ^{13}C NMR spectrum of TPP.

3. Characterization of host-guest interaction.

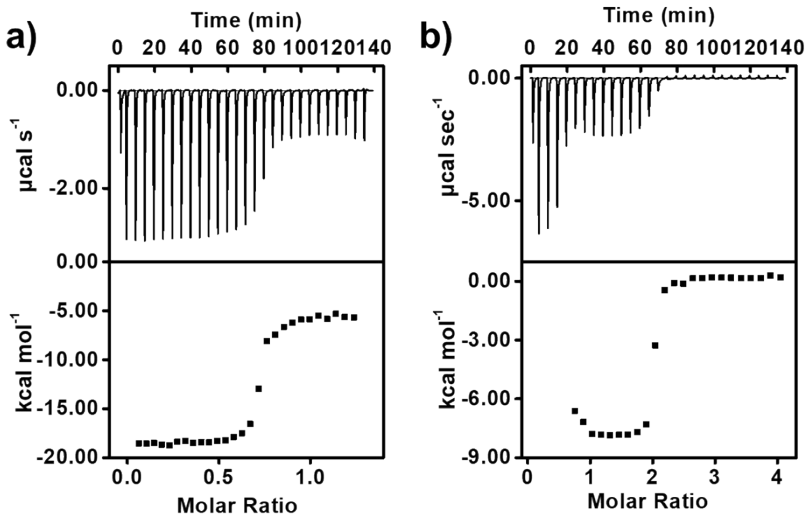

c)

TPP to CB[8]		
TPP to 3CB[8]@2TPP	K	$4.76 \times 10^6\ M^{-1}$
	ΔS	$-33.2\ K^{-1}\ cal^{-1}\ M^{-1}$
3CB[8]@2TPP to CB[8]@2TPP	K	$1.18 \times 10^7\ M^{-1}$
	ΔS	$8.14\ K^{-1}\ cal^{-1}\ M^{-1}$

Figure S5. ITC data for the titration of a) 0.50 mM TPP to 75 µM CB[8] and b) 1.00 mM TTP to 75 µM CB[8]. 10 mM PBS, pH = 7.4, 298.15 K. c) Thermodynamic data in the titration process.

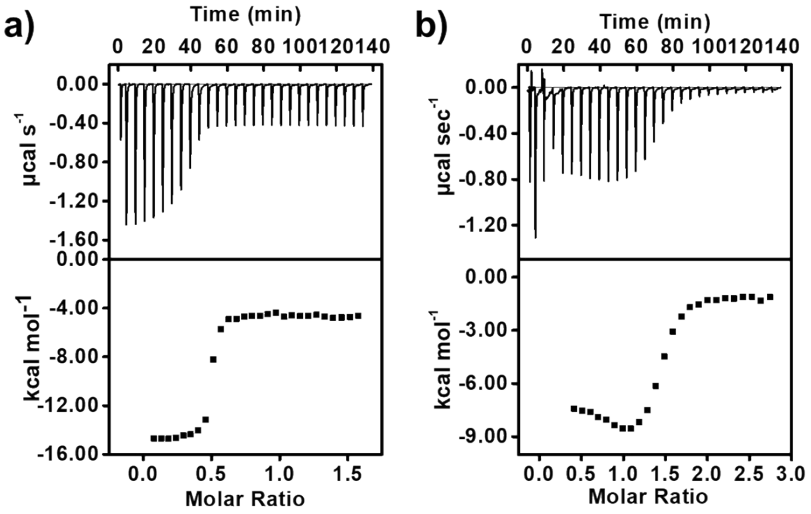

c)

CB[8] to TPP		
TPP to 2CB[8]@TPP	K	$2.00 \times 10^7\ M^{-1}$
	ΔS	$-15.0\ K^{-1}\ cal^{-1}\ M^{-1}$
CB[8]@2TPP to 3CB[8]@2TPP	K	$2.44 \times 10^6\ M^{-1}$
	ΔS	$0.60\ K^{-1}\ cal^{-1}\ M^{-1}$

Figure S6. ITC data for the titration of a) 0.30 mM CB[8] to 40 µM TPP and b) 0.30 mM CB[8] to 20 µM TPP. 10 mM PBS, pH = 7.4, 298.15 K. c) Thermodynamic data in the titration process.

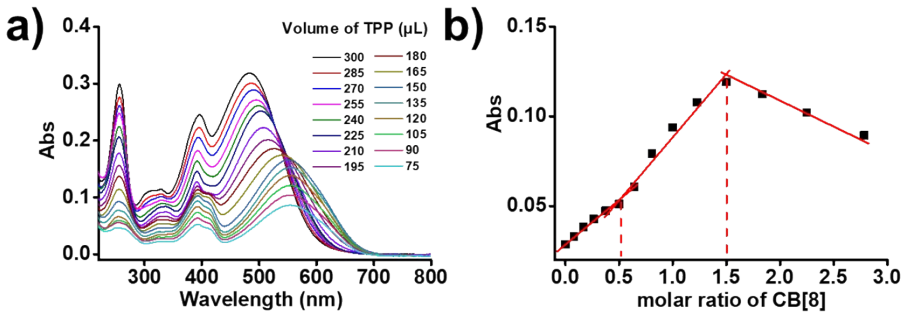

Figure S7. a) the absorption change with the decrease of TPP. b) The absorption at 600 nm with different molar ratio of CB[8]. [TPP]+[CB[8]] = 10 μM.

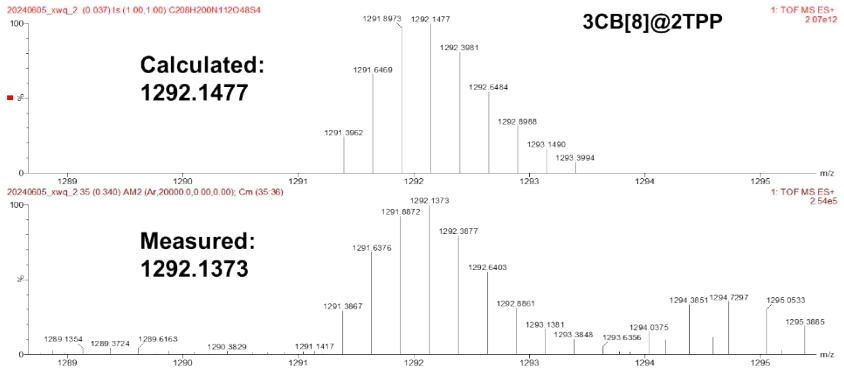

Figure S8. ESI-IT/TOF mass spectrum of 3CB[8]@2TPP.

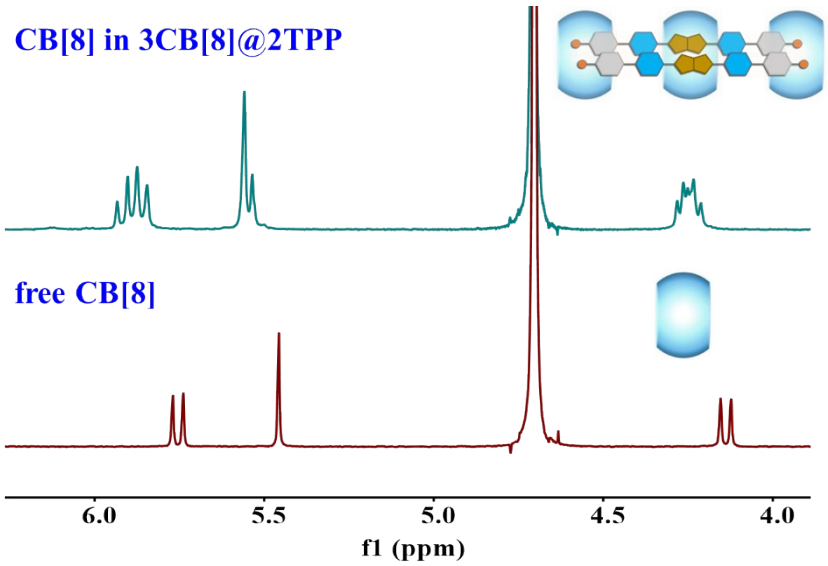

Figure S9. The proton signals of CB[8] in the host-guest complex or free state.

4. Photophysical and photochemical properties.

The fluorescence lifetime of 3CB[8]@2TPP is too short to be obtained in nanosecond scale.

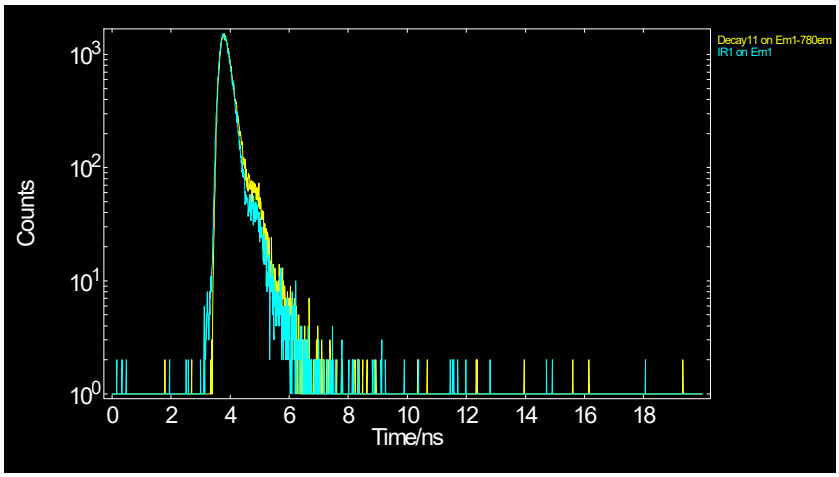

Figure S10. The fluorescence decay spectrum of 3CB[8]@2TPP in solution under air condition.

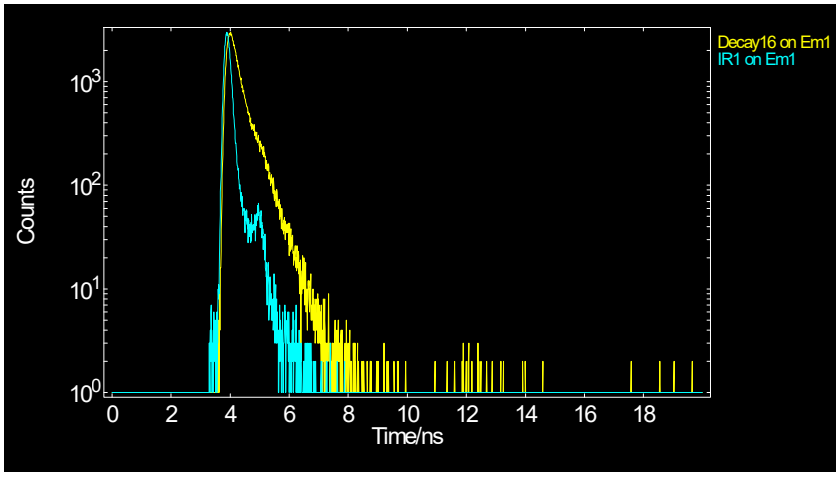

Figure S11. The fluorescence decay spectrum of 3CB[8]@2TPP in solid state.

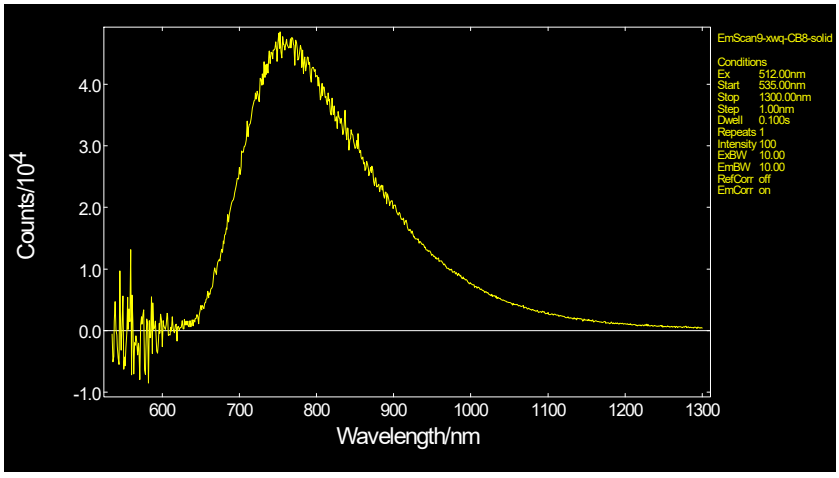

Figure S12. The fluorescence spectrum of 3CB[8]@2TPP in solid state.

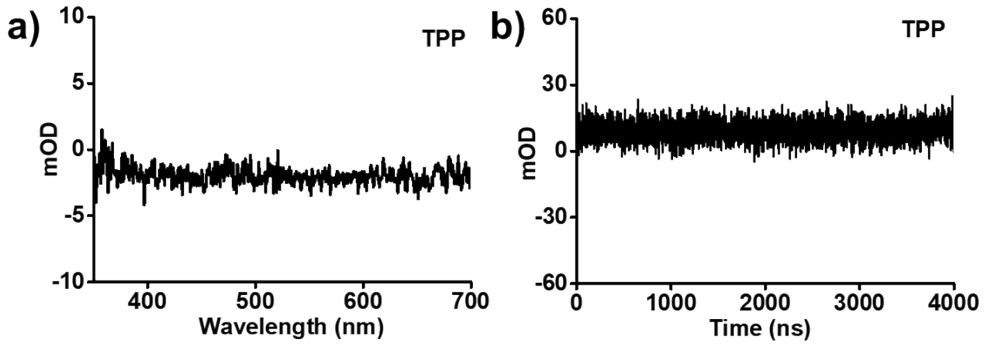

Figure S13. a) The transient absorption spectrum of TPP under N_2. b) The transient absorption decay curve at 450 nm. The delay time was 50 ns.

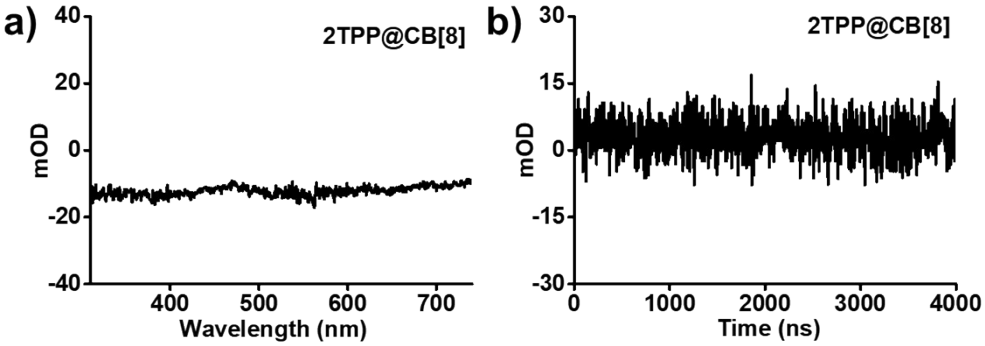

Figure S14. a) The transient absorption spectrum of CB[8]@2TPP under N_2. b) The transient absorption decay curve at 450 nm. The delay time was 50 ns.

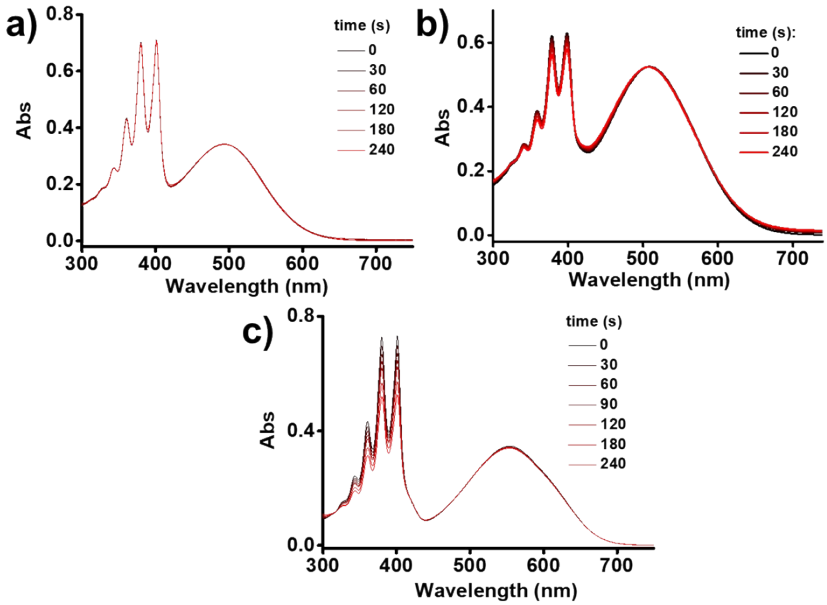

Figure S15. The absorption of ABDA in the presence of a) TPP, b) CB[8]@2TPP, and c) 3CB[8]@2TPP under the irradiation of 2W 520 nm light in air.

As shown in Figure S15&S16, the singlet oxygen yield ($^1O_2$) of 3CB[8]@2TPP was calculated by using rhodamine B (the $^1O_2$ yield is 78% in water) as the reference. 9,10-Anthracenediyl-bis(methylene)dimalonic acid (ABDA) was applied as the $^1O_2$ detector under the irradiation of 530 nm light. The equation to calculate $^1O_2$ yield is expressed as:

$$\frac{\emptyset_{sample}}{\emptyset_{standard}} = \frac{\left(-\frac{dlnA}{dt}\right)standard}{\left(-\frac{dlnA}{dt}\right)sample}$$

Finally, the singlet oxygen yield of 3CB[8]@2TPP was calculated to be 6.8%. As comparison, the singlet oxygen yield of CB[8]@2TPP was 1.9%, and free TPP did not have the ability to sensitize oxygen.

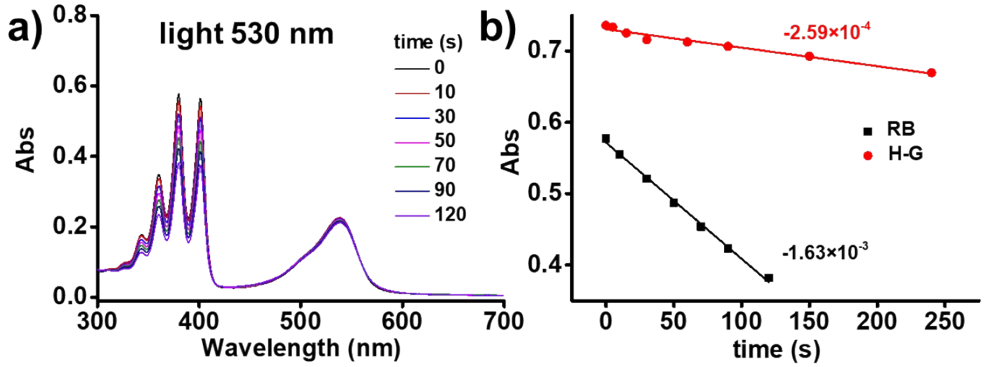

Figure S16. a) The absorption of ABDA in the presence of RB. b) The decay curve of ABDA at 380 nm in the presence of RB (black) and 3CB[8]@2TPP (red).

5. Aggregation effect of TPP.

As shown in Figure S17, temperature-dependent absorption experiments were carried out to investigate the aggregate phenomenon of TPP. With the temperature increasing from 5 to 55 °C, the absorption of TPP did not appear new band and the maximum absorption almost unchanged, indicating that TPP was existed without aggregation effect.

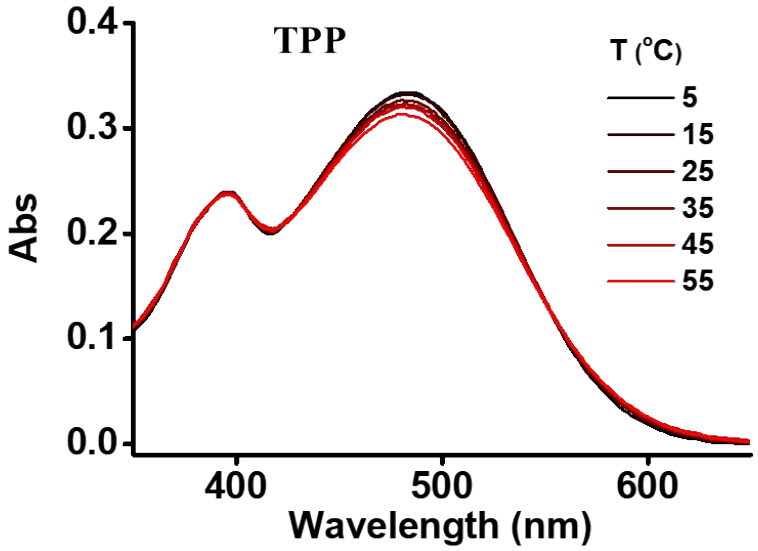

Figure S17. The absorption spectra of TPP at different temperature.

As shown in Figure S18, the absorption intensity of TPP had a linear relationship with the concentration, indicating the negligible aggregation effect.

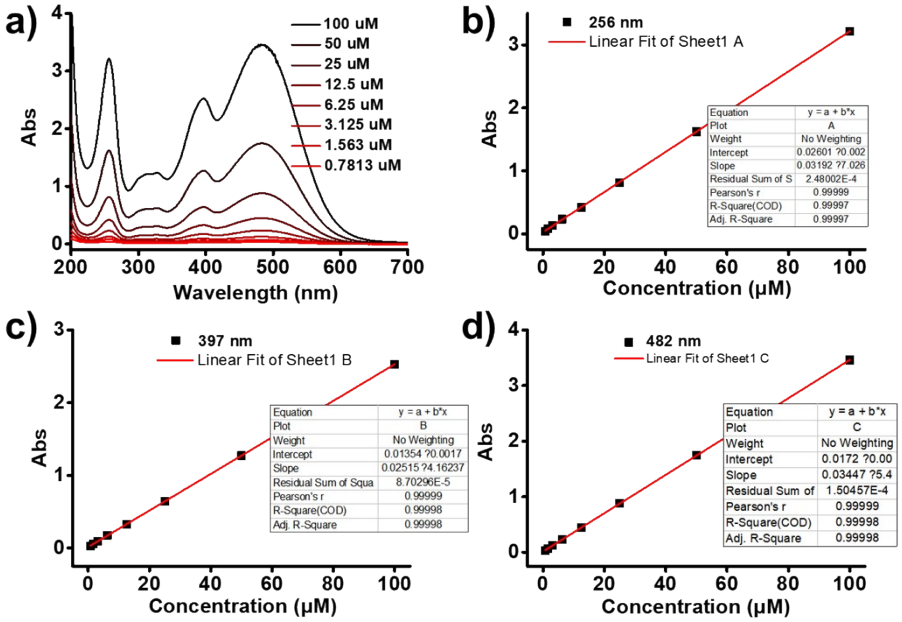

Figure S18. a) The absorption spectra of TPP at different concentrations. The absorption-concentration curves at b) 256 nm, c) 397 nm and d) 482 nm.

6. The stability of 3CB[8]@2TPP against temperature.

As shown in Figure S19, temperature-dependent absorption experiments were carried out to investigate the stability of 3CB[8]@2TPP. With the temperature increasing from 5 to 55 °C, the absorption of 3CB[8]@2TPP almost had no change, indicating its stability against temperature.

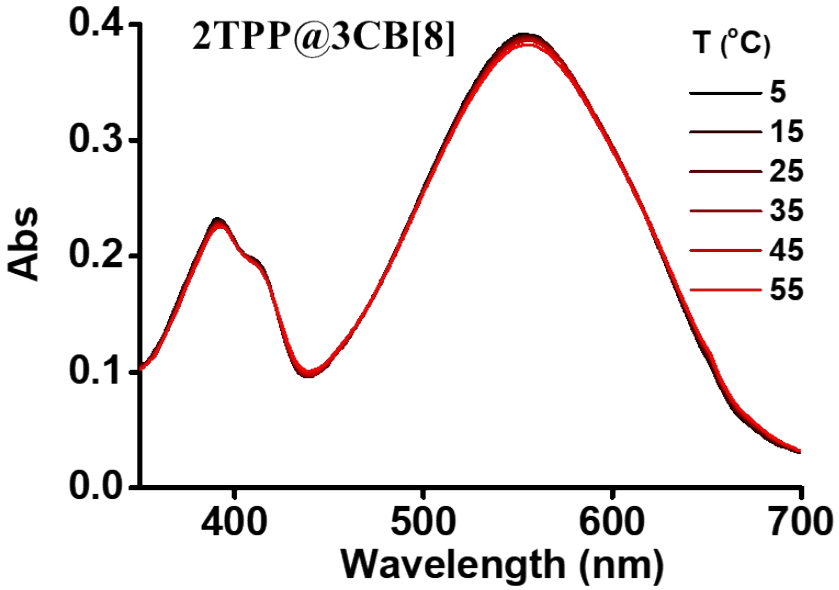

Figure S19. The absorption spectra of 3CB[8]@2TPP at different temperature.

7. Photocatalytic reactions.

7.1 Reaction conditions

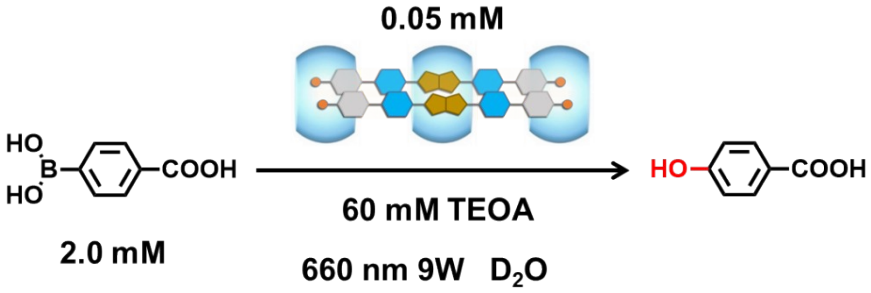

Figure S20. the oxidation of boronic acids catalyzed by 3CB[8]@2TPP.

7.2 Reaction catalyzed by CB[8]@2TPP or TPP.

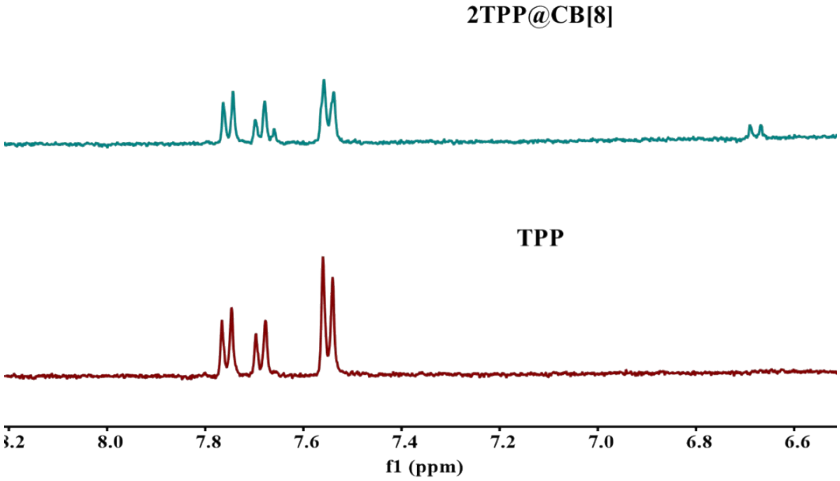

Figure S21. The ^{1}H NMR spectra of CPBA catalyzed by CB[8]@2TPP or TPP.

7.3 Substrate diversity.

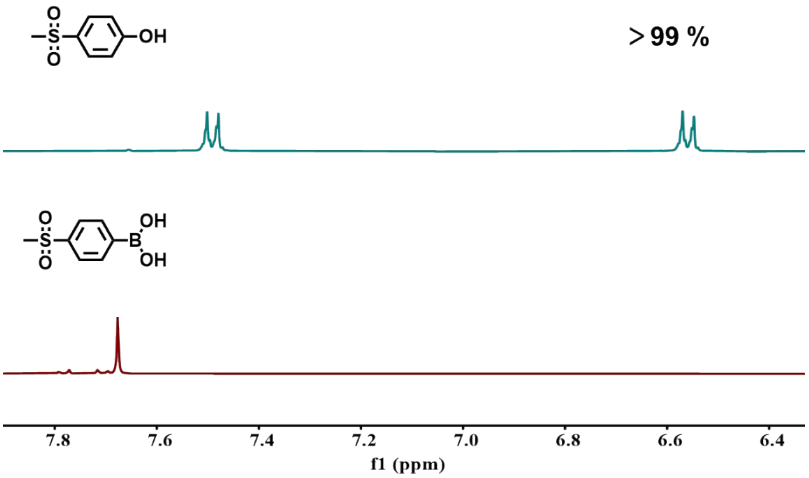

Figure S22. The ^{1}H NMR spectra of 4-(methylsulfonyl)benzeneboronic acid catalyzed by 3CB[8]@2TPP.

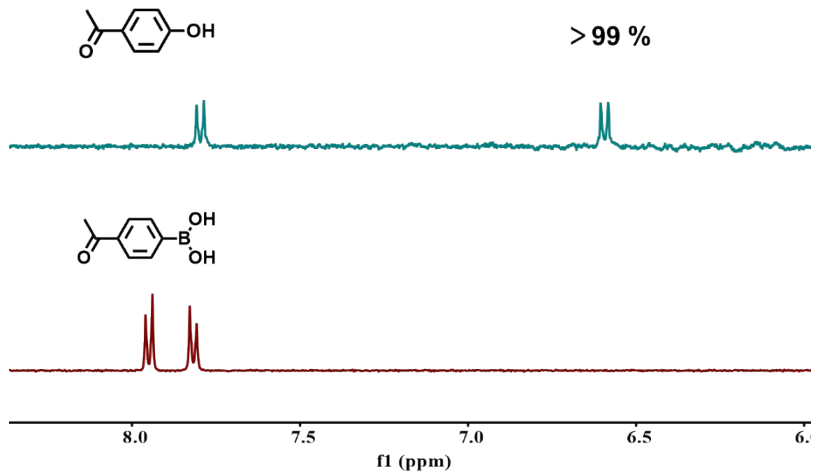

Figure S23. The ^{1}H NMR spectra of 4-acetylphenylboronic acid catalyzed by 3CB[8]@2TPP.

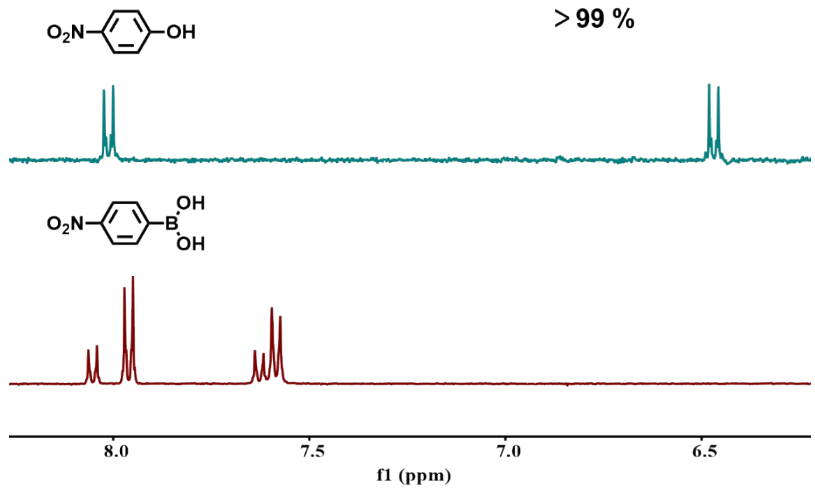

Figure S24. The ^{1}H NMR spectra of 4-nitrophenylboronic acid catalyzed by 3CB[8]@2TPP.

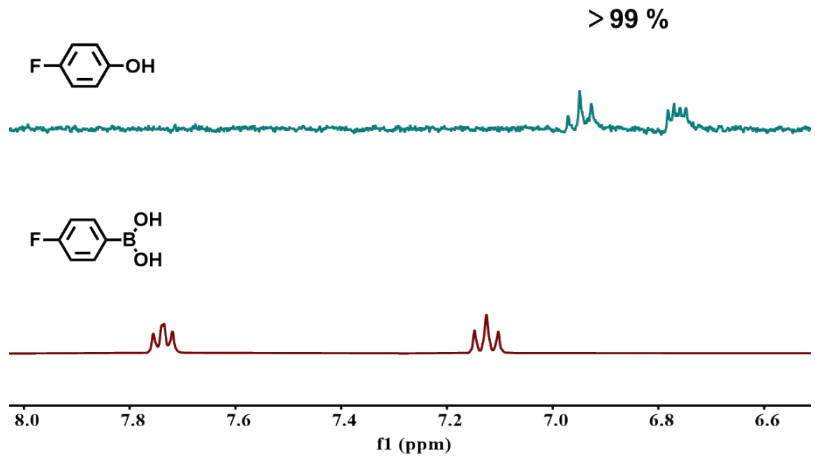

Figure S25. The ^{1}H NMR spectra of 4-fluorobenzeneboronic acid catalyzed by 3CB[8]@2TPP.

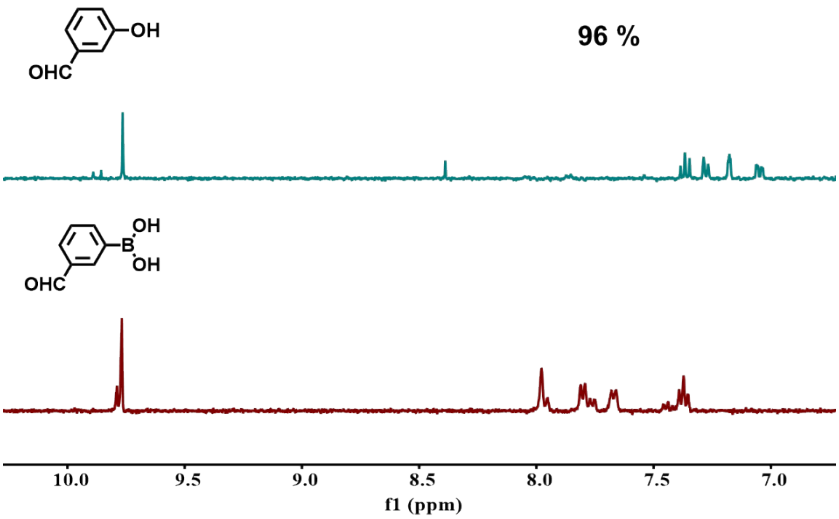

Figure S26. The ^{1}H NMR spectra of 3-formylphenylboronic acid catalyzed by 3CB[8]@2TPP.

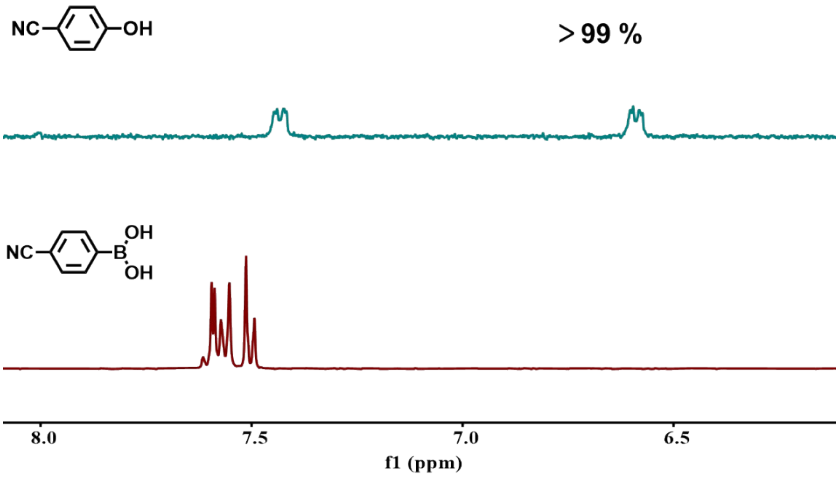

Figure S27. The ^{1}H NMR spectra of 4-cyanophenylboronic acid catalyzed by 3CB[8]@2TPP.

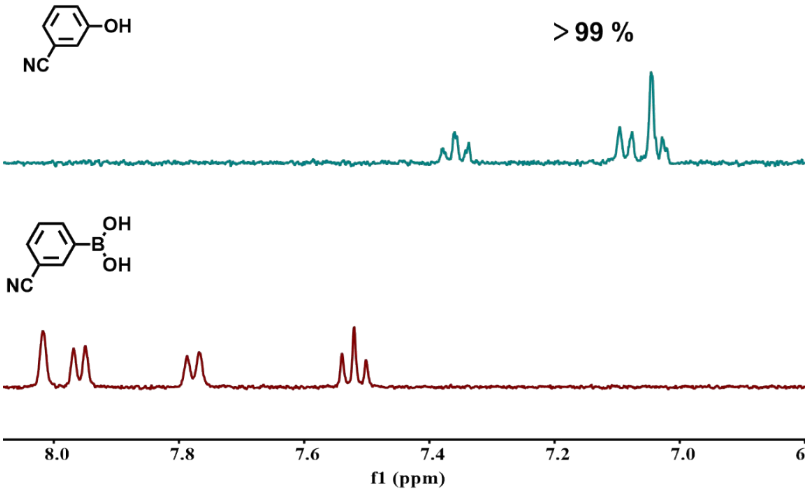

Figure S28. The ^{1}H NMR spectra of 3-cyanophenylboronic acid catalyzed by 3CB[8]@2TPP.

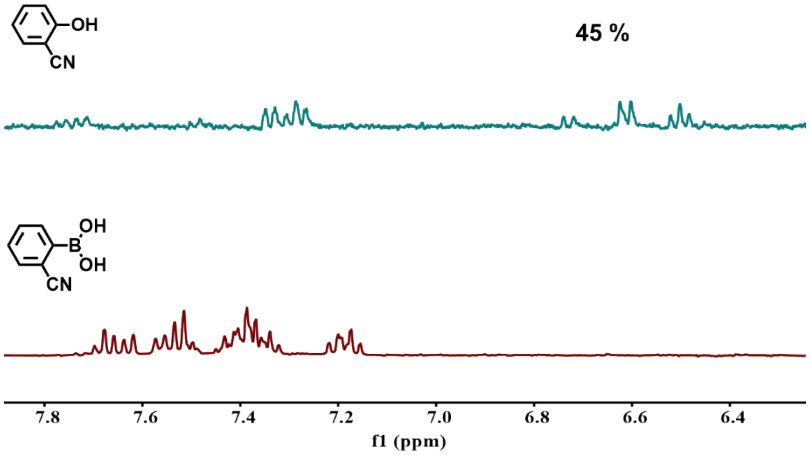

Figure S29. The ^{1}H NMR spectra of 2-cyanophenylboronic acid catalyzed by 3CB[8]@2TPP.

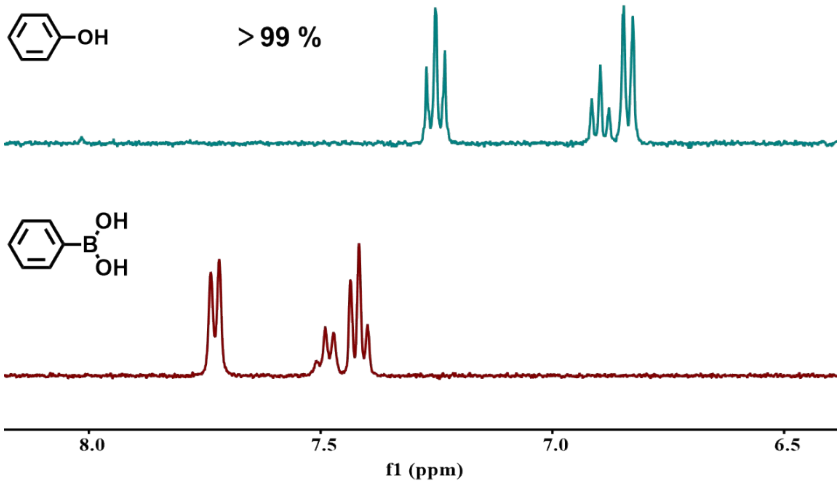

Figure S30. The ^{1}H NMR spectra of phenylboronic acid catalyzed by 3CB[8]@2TPP.

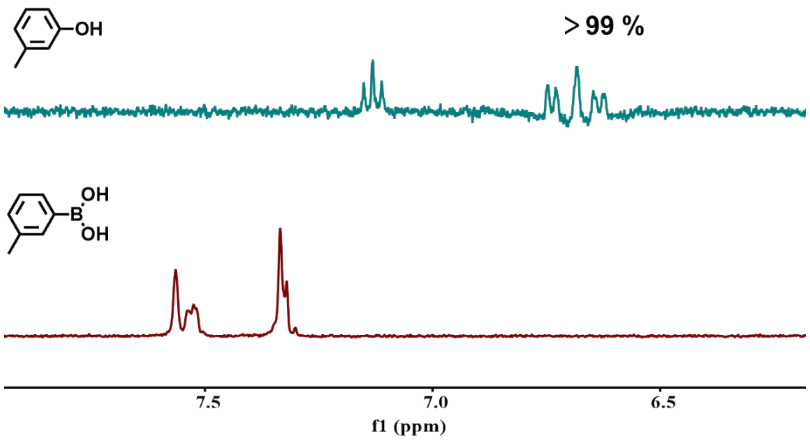

Figure S31. The ^{1}H NMR spectra of 3-tolylboronic acid catalyzed by 3CB[8]@2TPP.

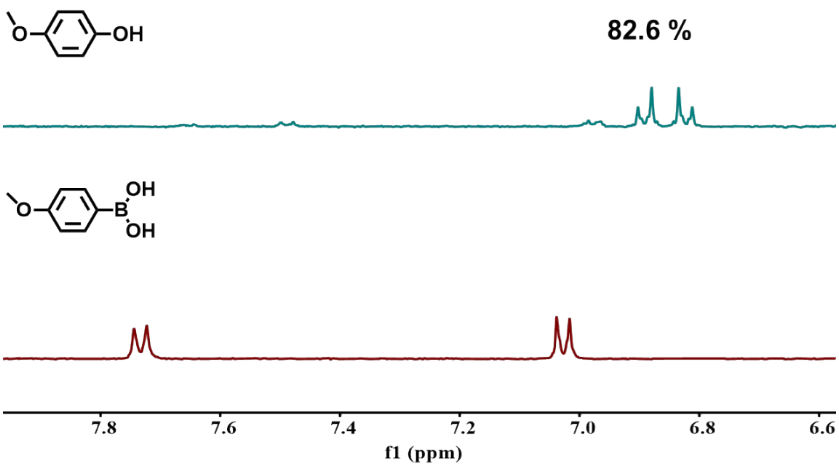

Figure S32. The ^{1}H NMR spectra of 4-methoxyphenylboronic acid catalyzed by 3CB[8]@2TPP.

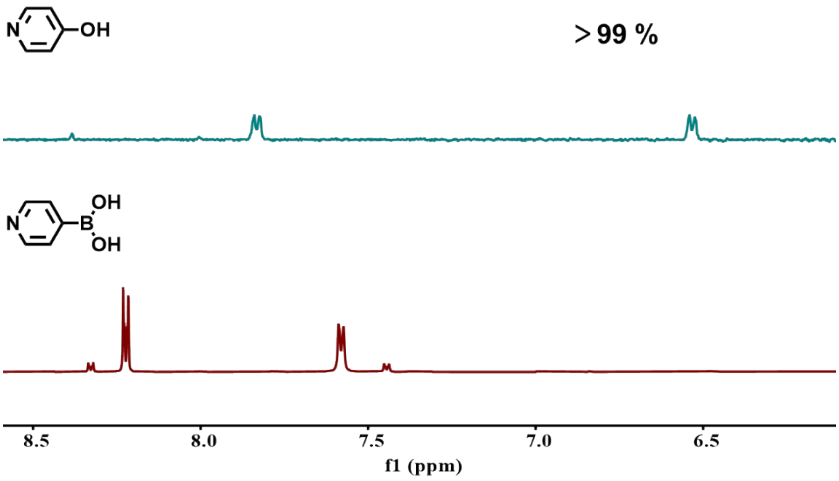

Figure S33. The ^{1}H NMR spectra of pyridine-4-boronic acid catalyzed by 3CB[8]@2TPP.

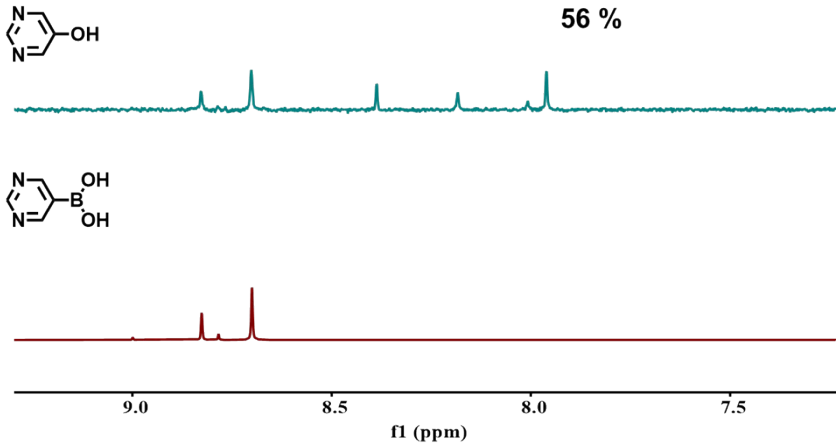

Figure S34. The ^{1}H NMR spectra of 5-pyrimidinylboronic acid catalyzed by 3CB[8]@2TPP.

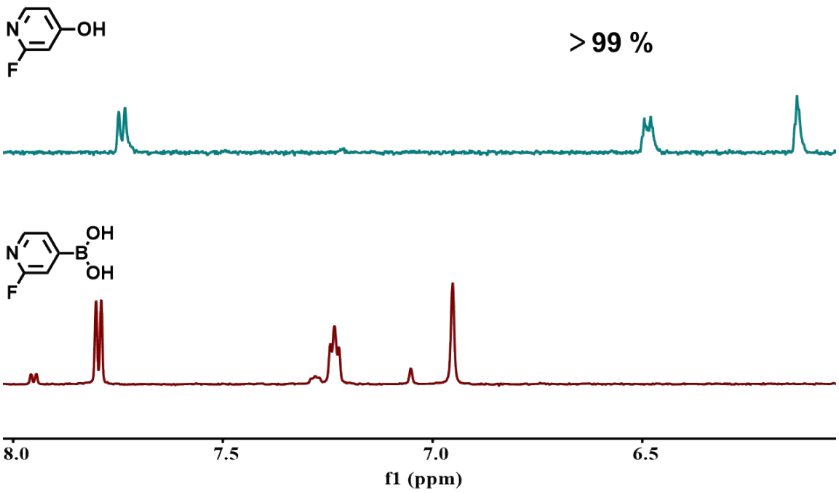

Figure S35. The ^{1}H NMR spectra of 2-fluoropyridine-4-boronic acid catalyzed by 3CB[8]@2TPP.

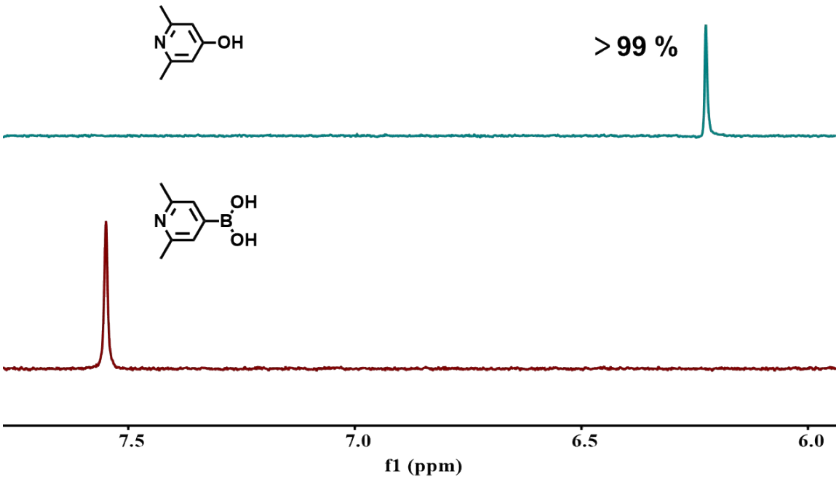

Figure S36. The ^{1}H NMR spectra of 2,6-dimethyl-pyridine-4-boronic acid catalyzed by 3CB[8]@2TPP.

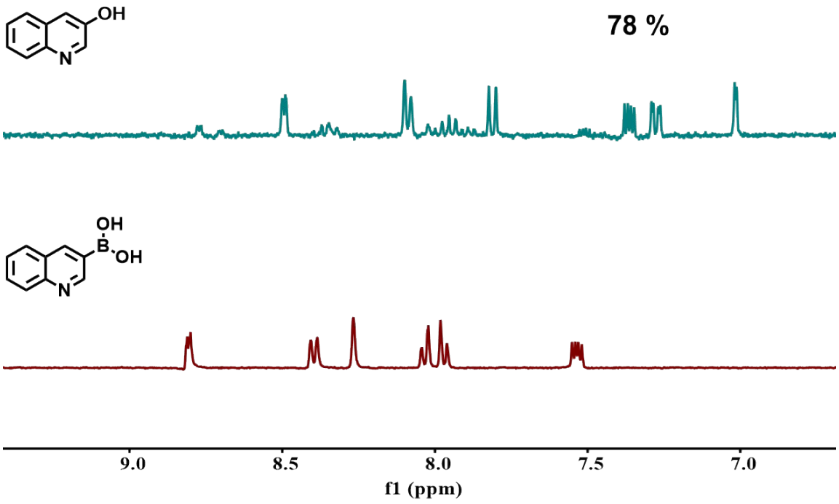

Figure S37. The ^{1}H NMR spectra of 3-quinolinyl-boronic acid catalyzed by 3CB[8]@2TPP.

References:

[1] J. Luo, B. Hu, C. Debruler and T. L. Liu, A π-conjugation extended viologen as a two-electron storage anolyte for total organic aqueous redox flow batteries, *Angew. Chem. Int. Ed.*, 2018, **57**, 231-235.